COMPARISONS BETWEEN NUMERICAL CALCULATIONS AND MEASUREMENTS IN THE VANED DIFFUSOR OF SHF IMPELLER

Annie-Claude Bayeul-Lainé[1,]*, Patrick Dupont[2], Patrick Cherdieu[2], Antoine Dazin[1], Gérard Bois[1], Olivier Roussette[1]

[1]LML, UMR CNRS 8107, Arts et Metiers PARISTECH, 8, boulevard Louis XIV 59046 LILLE Cedex, France
[2] LML, UMR CNRS 8107, Ecole Centrale de Lille

**corresponding author: ☎+333 20 62 39 04, Fax +333 20 53 55 93*
E-mail address: annie-claude.bayeul-laine@ensam.eu

Abstract

The paper presents analysis of the performance and the internal flow behaviour in the vaned diffusor of a radial flow pump using PIV technique and pressure probe traverses.
PIV measurements have been performed at mid height inside one diffusor channel passage for a given speed of rotation and various mass flow rates. For each operating condition, PIV measurements have been made for different angular positions of the impeller. For each angular position, instantaneous velocities charts have been obtained on two simultaneous views, which allows, firstly ,to cover the space between the leading edge and the diffusor throat and secondly, to get a rather good evaluation of phase averaged velocity charts and "fluctuating rates ". Probe traverses have been performed using a 3 holes pressure probe from hub to shroud diffusor width at different radial locations in between the two diffusor geometrical throats.
The numerical simulations were realized with the commercial codes: i-Star CCM+ 7.02.011, ii-CFX. Frozen rotor and fully unsteady calculations of the whole pump were performed.
Comparisons between numerical and experimental results are presented and discussed for one mass flow rate. In this respect, the effects of fluid leakage due to the gap between the rotating and fixed part of the pump model are analysed and discussed.

1. Introduction

Flow behaviour in a radial machine is quite complex and is sometime strongly depending on rotor stator interactions and operating conditions.
In numerical simulation, two aspects have to be considered, the first one concerns the governing equations which are solved in the model: two kinds of numerical calculations are currently used in turbomachinery (i-frozen rotor calculations, ii-unsteady calculations). The second aspect concerns the geometrical model. Some geometrical simplifications are currently used. For example, the leakage flows are often neglected. It is obvious that a complex model (fully unsteady, with leakage flows) will be more time consuming but closer to the real physics. The aim of the paper is to point out the limits of the numerical models. To do so, several numerical calculations are compared to experimental results.
The test model corresponds to the so-called SHF pump, working with air, in similarity conditions compared to water, for which several publications have been made [1 to 6 for example] for numerical and PIV comparisons. Several investigations have been recently performed on this test bench using PIV [3, 4 8]. The existing database has been completed by pressure probe measurements for a complete flow performance analysis. These measurements are compared to several numerical calculations in the present paper.

2. Experiments

2.1. Test and apparatus

Test pump model and PIV measurements conditions have been already described in several papers as ref [3, 4, 5 and 6] and main geometrical characteristics as well as operating conditions are given in table 1. This set-up allows the existence of a "positive" leakage flow going into the gap between impeller outlet section and inlet vaned diffusor section which is specific to the experimental set-up. This is due to the fact that the pump outlet pressure corresponds to atmospheric conditions.

2.2. Three-holes pressure probe

Figure 1: picture and sketch of the three-hole pressure probe

A three holes probe (fig 1) has been used to make hub to shroud traverses in the same planes where wall static pressures are measured. Using a specific calibration one can

get total pressure, static pressure, absolute velocity and its two components in radial and tangential direction.

2.3. General Flow conditions

All types of measurements have been performed for several mass flow rates. But, results presented in this paper refer only to one mass flow rate corresponding to the design point of the vaned diffusor Q/Q_{ni}=0.766, which is different to impeller design mass flow rate Q/Q_{ni}=1. This vaned diffusor design was chosen in order to allow an enlarge pump performance characteristic curve for low mass flow rates.

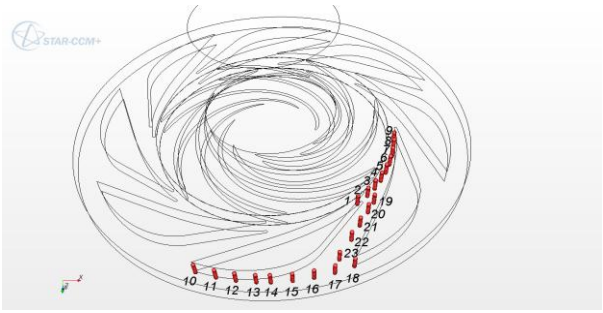

Figure 2: Diffusor measurement locations for probe traverse and unsteady calculations

In order to well represent the flow field, twenty-three location positions are defined as it can be seen in figure 2. For each location, ten axial positions are registered (b*=0.125, 0.2, 0.25, 0.375, 0.5, 0.625, 0.75, 0.875, 0.925, 0.975). The present analysis focuses only on locations 19 to 23 in the blade to blade channel of the diffuser.

3. Calculations

Calculations were performed using Star CCM+ code and results are compared with CFX results already published [7]

3.1. Frozen rotor calculations (Star CCM+)

Three-dimensional steady incompressible Reynolds averaged Navier–Stokes equations are solved. The SST k-ω turbulence model is used [8].

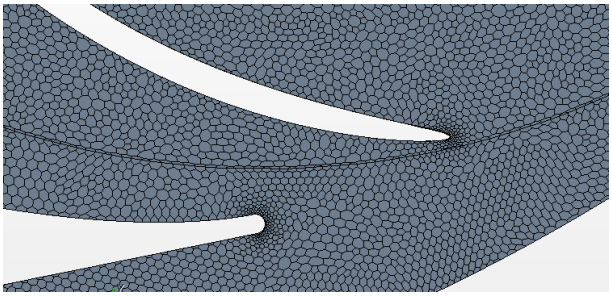

Figure 3: Local mesh between Impeller and diffusor

The calculation domain was divided into three zones: the inlet zone, the impeller zone and the diffusor zone.

The boundary condition at the inlet consisted of a mass flow rate (0.305 kg/s; Q/Q_{ni}=0.766). The boundary condition at the outlet was the atmospheric pressure (0 Pa). The fluid (air) was considered incompressible at a constant temperature of 20ºC.

A polyhedral mesh with prism layers is used for all calculations (5 prism layers for a total prism layer thickness of 1 mm). The target size is 3 mm and the minimum size 0,5 mm . The size of the grid is about 3. 10^6 cells. A sketch of local mesh is given in figure 3.

Line probes are plotted in the whole domain: Each probe is duplicated seven times in order to obtain all parameters (pressure, total pressure, radial, tangential and axial velocity and velocity magnitude) for different relative positions of the diffusor comparatively to the impeller (figure 4). This is equivalent to azimuthal positions equal to n* 360/(Zi*Zd) with n=0,1 ,2, 3, 4, 5, 6 and 7.

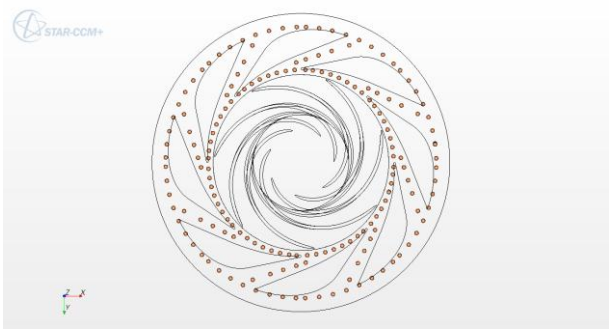

Figure 4: Diffusor measurement locations for probe traverse and frozen rotor calculations

3.2. Unsteady calculations

3.2.1. Star CCM+

Table 1: pump parameters

Entry duct	
Diameter	0.14113 m
length	0.25 m
Impeller	
Inlet radius	0.14113 m
Outlet radius	0.2549 m
Number of blades	Z_i=7
Outlet height	0.04 m
Impeller design flow rate	Q_{ni}=0.337m^3/s
Rotation speed	N=1710 rpm
Diffusor	
Inlet radius	0.2549 m
Outlet radius	0.44 m
Number of vanes	Z_d=8
Height	0.04 m
Diffusor design flow rate	Q_{nd}=0.8Q_{ni}

The unsteady calculations were realized with the same mesh. The convergence criteria are less than $1.e^{-4}$. Maximum values of y+ are around 15, and mainly below 9 in the whole computational domain as can be seen in Figure 5.

A time step of 4,87 10^{-5} s, corresponding to an angular rotation of 0,5°, has been chosen.

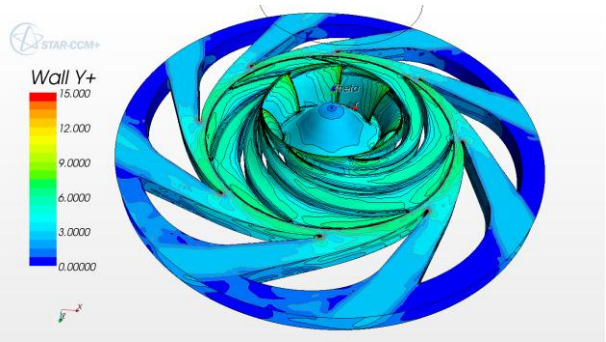

Figure 5: y+ for unsteady calculations

3.2.2. CFX

In order to investigate the influence of leakage flows, numerical results obtained using CFX [7] are also presented. G. Cavazzini et al [7] proposed two kinds of unsteady simulations, with and without leakage flows.

4. Results and Comparisons

4.1. Global performances

Global results of total theoretical head pump are in good agreement between EULER one dimensional approach and frozen rotor calculation. Unsteady calculation results, performed for the non-dimensional mass flow rate Q*=0,766, give the same level, as it can be seen in figure 6. Comparison between real total head curve obtained by calculations and experiments are also given in the same figure. One has to note that pump mass flow rates are higher than impeller mass flow rates due to "positive" leakage flow. This is the reason why the experimental head pump is higher than the numerical total pump head coefficient.

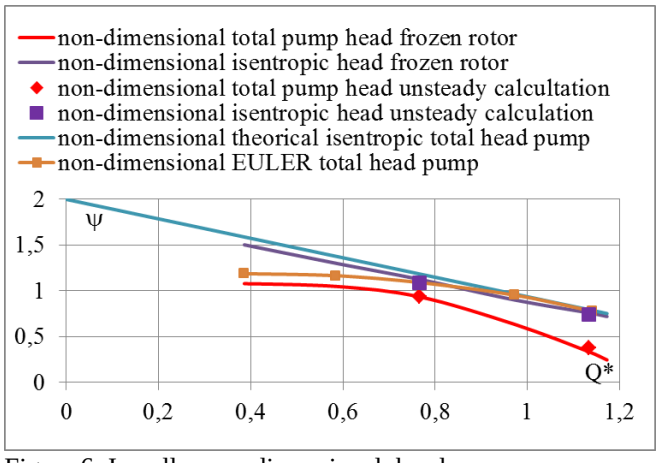

Figure 6: Impeller non-dimensional head curve

$$Q^* = \frac{Q}{Q_n} \qquad (1)$$

Non-dimensional calculated total head is defined by equation (2) and non-dimensional isentropic head by equation (3)

$$\psi_{tc} = \frac{dp_t}{\rho U_2^2/2} \qquad (2)$$

$$\psi_{ti} = \frac{C\Omega}{Q_m U_2^2/2} \qquad (3)$$

4.2. Hub-to-shroud local flow characteristics.

The results obtained at location 19 has been chosen to compare frozen rotor and unsteady calculations,. Numerical results are shown in figures 7 and 8 respectively for frozen rotor and unsteady calculations. Radial velocity distributions depend on the relative impeller blade position compared with vaned diffusor ones as shown in figure 7, whereas only time acts for unsteady results. Unsteady calculations give smoother hub to shroud gradients and less difference between blade to blade results.

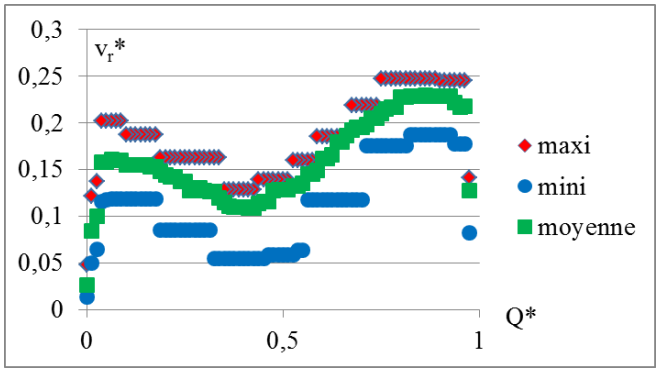

Figure 7: hub-to-shroud non-dimensional radial velocity in different blade to blade channels for probe 19 (frozen rotor calculation)

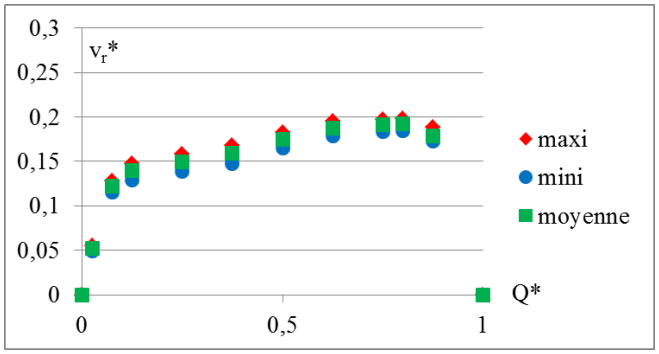

Figure 8: hub-to-shroud non-dimensional radial velocity in different blade to blade channels for probe 19 (unsteady calculation)

Local numerical results of frozen rotor calculations without leakage ("CCM+ 1"), unsteady calculations without leakage (obtained from two different codes: "CCM+ 2" and "CFX 1"), and unsteady calculations with leakage (obtained only from CFX [7]: "CFX 2") are presented in figures 9 to 12. PIV measurements ("PIV"), wall static pressure ("ps") and three-holes pressure probes ("probes") results are plotted on the same figures.

Figure 9a

location19

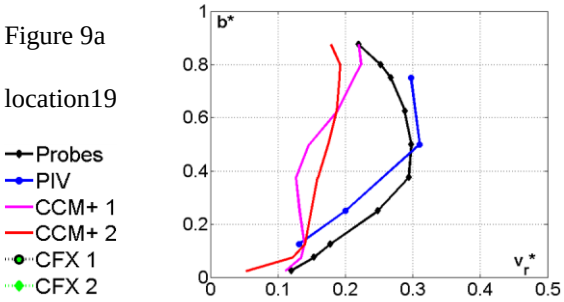

Figure 9b

location20

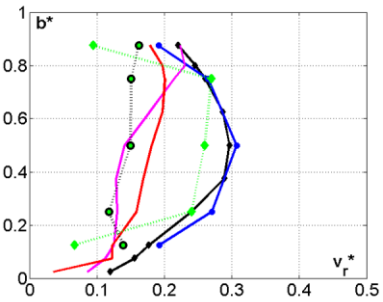

Figure 9c

location21

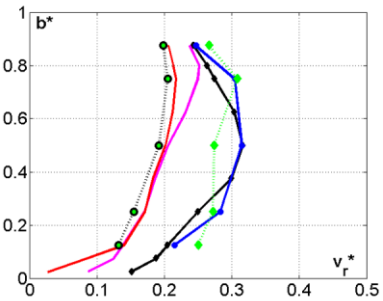

Figure 9d

location22

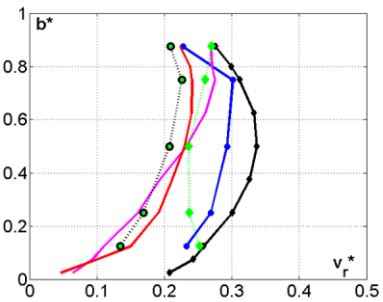

Figure 9e

location23

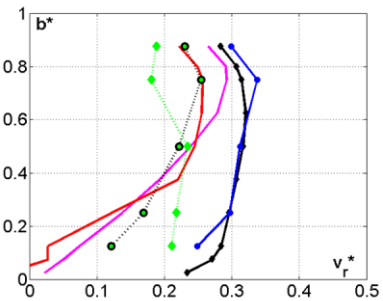

Figures 9a to 9e : Hub-to-shroud non-dimensional radial velocity v_r^* from different location inside the diffusor channel

Figure 10a

location19

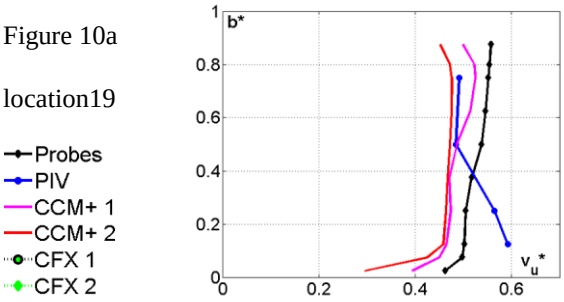

Figure 10b

location20

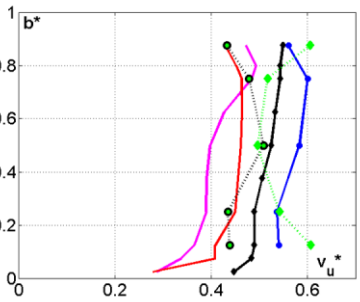

Figure 10c

location21

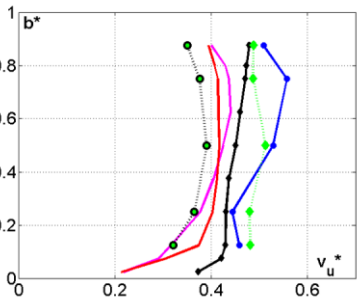

Figure 10d

location22

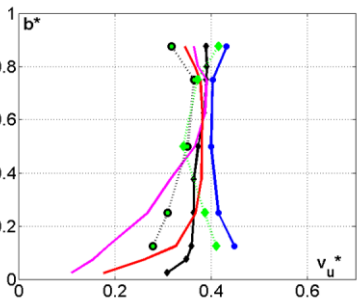

Figure 10e

location23

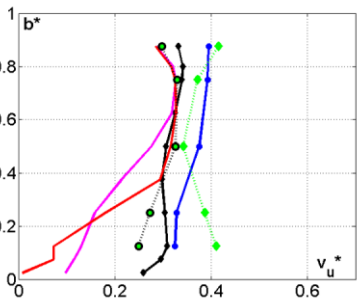

Figures 10a to 10e : Hub-to-shroud non-dimensional radial velocity v_u^* from different location inside the diffusor channel

Figure 11a

location19

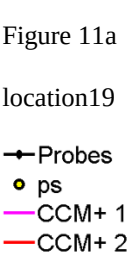

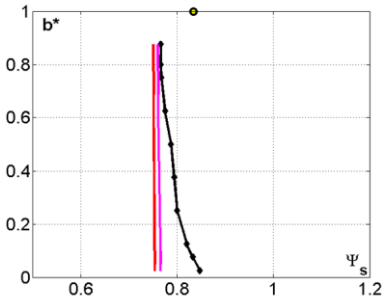

Figure 11b

location20

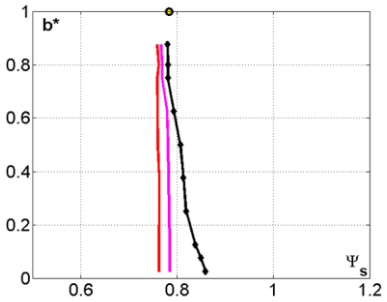

Figure 11c

location21

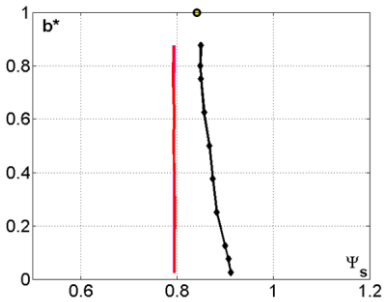

Figure 11d

location22

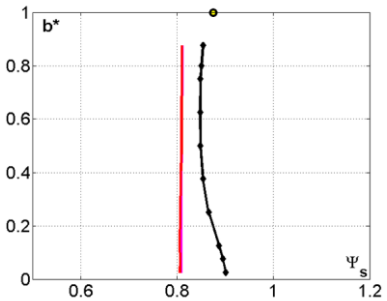

Figure 11e

location23

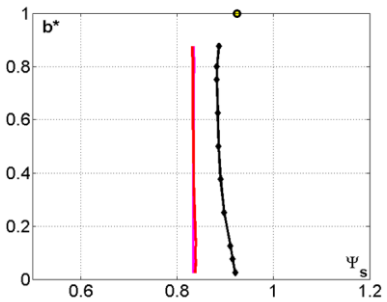

Figures 11a to 11e : Hub-to-shroud non-dimensional Pressure Ψ_s from different location inside the diffusor channel 2

Figure 12a

location19

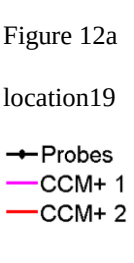

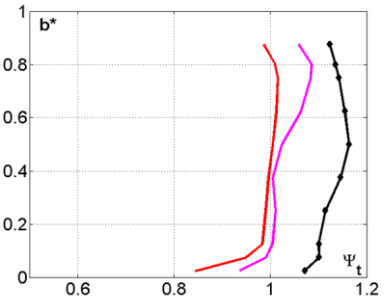

Figure 12b

location20

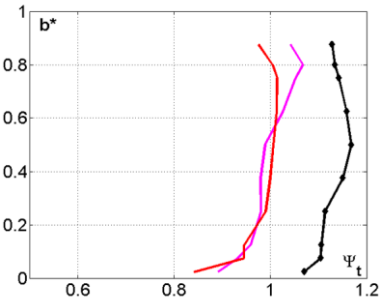

Figure 12c

location21

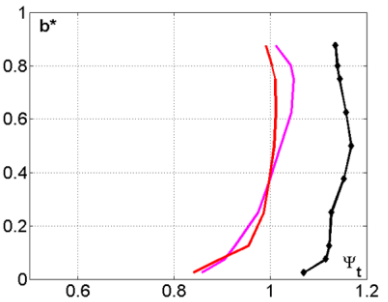

Figure 12d

location22

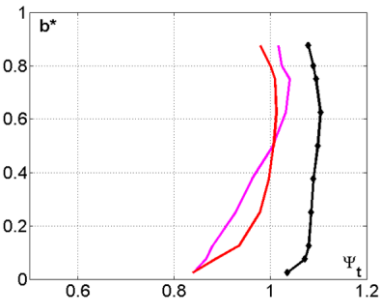

Figure 12e

location23

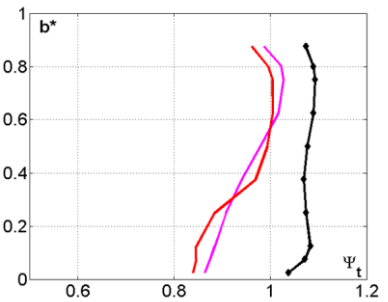

Figures 12a to 12e : Hub-to-shroud non-dimensional total pressure Ψ_t from different location inside the diffusor channel

These experimental results have been performed with pump configuration with leakage. Results present radial and tangential velocities, static and total pressures distribution from hub to shroud section and for several channel locations as already shown in figure 2.

The influence of leakage can be easily seen when comparing numerical results obtained without and with leakage. Experimental results are in good agreement with calculations obtained with leakage. This can be mainly seen on radial velocity distribution shown in figure 9. These results must be more deeply analysed, in particular PIV ones; they strongly depend on impeller position during its rotation and only time-averaged values are presented here. Pressure probe results are also depending on unsteady effects and this has to be taken into account for further data reduction analysis.

The influence of leakage can also be seen, looking at pressure distributions in the diffusor. Static pressure recovery is better with leakage (figure 11). Total pressure probe results show higher levels compared with calculations without leakage and also show that leakage effects acts mainly near shroud section preventing separation in location 22 and 23.

5. Conclusions

Comparisons between numerical frozen rotor assumption and fully unsteady calculations show that global performances can be obtained with frozen rotor assumption but that local values must be analysed with unsteady results even in the vaned diffusor far from impeller outlet section.

Results issued from different numerical approaches and experiments coming from PIV and pressure probe have been presented and compared. The pump model configuration allows leakage to be an important parameter that has to be taken into account in order to make good comparisons between numerical and experiments.

Nomenclature

b	Impeller or diffuser width	(m)
C	Impeller moment	(mN)
H	Total pump head	(m)
N	Rotation speed	(rpm)
p	Pressure	(Pa)
p_t	Total pressure	(Pa)
Q	Volume flow rate in impeller	(m^3/s)
Q_m	Mass flow rate in impeller	(kg/s)
Q_n	Nominal volume flow rate	(m^3/s)
R_i	Radius of section i	(m)
v_r	Radial velocity	(m/s)
$v_r^*=v_r/U_2$	Non-dimensional radial velocity	
v_u	Tangential velocity	(m/s)
$v_u^*=v_u/U_2$	Non-dimensional tangential velocity	
v_z	Axial velocity	(m/s)
$v_z^*=v_z/U_2$	Non-dimensional axial velocity	
$U_2=\Omega*R_2$	Frame velocity at impeller outlet	(m/s)
Z_i	Number of impeller blades = 7	
Z_d	Number of diffusor blades = 8	
ρ	Air density	(kg/m^3)
Θ	Azimuthal vane blade angle	(°)
Ω	Angular Velocity	(rad/s)
Ψ_{tc}	Non-dimensional total pump head	
Ψ_{ti}	Non-dimensional isentropic head	

Index

1	Impeller inlet
2	Impeller outlet
3	Diffusor outlet
c	calculated
d	diffusor
i	Impeller or isentropic

Acknowledgements

The authors wish to thank Region Nord- Pas de Calais and CNRS for their financial support in the frame of the CISIT program and Mrs Giovanni Cavazzini (University of Padova) for extended data reduction results [7].

References

[1] N. Arndt, A.J. Acosta, C.E. Brennen, T.K. Caughey, Experimental investigation of rotor-stator interaction in a centrifugal pump with several diffusors, *Journal of Turbomachinery*, ing. Vol 112, 1990, pp 98-108

[2] K. Eisele, Z. Zhang, M.V. Casey, J. Gûlich, Schechenmann, Flow analysis in a pump difffuser Part 1: LDA and PTV measurements of the unsteady flow, *ASME Journal of Fluids Engineering*, Vol. 119, 1997

[3] G. Wuibaut, P. Dupont, G. Caignaert, M. Stanislas, 2000, Experimental analysis of velocities in the outlet part of a radial flow pump impeller and the vaneless diffusor using particle image velocimetry, *XX IAHR Symposium*, Charlotte, USA, 6-9 August

[4] G. Wuibaut, G. Bois, M. El Hajem, A. Akhras, J.Y. Champagne, Optical PIV and LDV Comparisons of Internal Flow Investigations in SHF Impeller, *Int. J. of Rotating Machinery*, 1-9, 2006

[5] A. Dazin, O. Coutier-Delgosha, P. Dupont, S. Coudert, G. caignaert, G. Bois, Rotating stall in the vaneless of a radial flow pump, *Procceedings of the 8th iInternational Symposium on Experimental and Computational Aerothermodynamics of Internal Flows*, Lyon, July 2007, paper ISAIF8-00102

[6] G. Cavazzini, P. Dupont, G. Pavesi, A. Dazin, G. Bois, A. Atif, P. Cherdieu, Analysis of unsteady flow velocity fields inside the impeller of a radial flow pump : PIV measurements and numerical calculation comparisons, *Proc. of ASME-JSME-HSME Joint fluids engineering conference 2011*, July 24-29, 2011, Hamamatsu, Japan

[7] G. Cavazzini, G. Pavesi, G. Ardizzon, P. Dupont, S. Coudert, G. Caignaert, G. Bois Analysis of the rotor-stator interaction in a radial flow pump 2009 *Houille blanche – revue internationale de l'eau*

[8] Menter FR Two-equation eddy-viscosity turbulence modeling for engineering applications 1994 *AIAA Journal* **32(8)** pp. 1598-1605